Article published online: 2024-07-12

Diagnostic Imaging Performance of Dual-Energy Computed Tomography Compared with Conventional Computed Tomography and Magnetic Resonance Imaging for Uterine Cervical Cancer

Saki Shibuki[1] Tsukasa Saida[2] Kensaku Mori[2] Toshitaka Ishiguro[2] Taishi Amano[1] Miki Yoshida[1] Mariko Miyata[3] Toyomi Satoh[4] Takahito Nakajima[2]

[1] Department of Radiology, University of Tsukuba Hospital, Tsukuba, Ibaraki, Japan
[2] Department of Radiology, Institute of Medicine, University of Tsukuba, Tsukuba, Ibaraki, Japan
[3] Department of Radiology Technology, University of Tsukuba Hospital, Tsukuba, Ibaraki, Japan
[4] Department of Obstetrics and Gynecology, Institute of Medicine, University of Tsukuba, Tsukuba, Ibaraki, Japan

Address for correspondence Tsukasa Saida, MD, Department of Radiology, Institute of Medicine, University of Tsukuba, 1-1-1 Tennodai, Tsukuba, Ibaraki 305-8575, Japan (e-mail: saida_sasaki_tsukasa@md.tsukuba.ac.jp).

Indian J Radiol Imaging

Abstract

Objective This article evaluates the ability of low-energy (40 keV) virtual monoenergetic images (VMIs) in the local diagnosis of cervical cancer compared with that of conventional computed tomography (C-CT) and magnetic resonance imaging (MRI), using clinicopathologic staging as a reference.

Methods This prospective study included 33 patients with pathologically confirmed cervical cancer who underwent dual-energy CT and MRI between 2021 and 2022. The contrast-to-noise ratio (CNR) of the tumor-to-myometrium was compared between C-CT and VMI. Additionally, sensitivity, specificity, and area under the receiver operating characteristic curve (AUC) for each local diagnostic parameter were compared between C-CT, VMI, and MRI. Interradiologist agreement was also assessed.

Results The mean CNR was significantly higher on VMI ($p = 0.002$). No significant difference in AUC was found between C-CT and VMI for all local diagnostic parameters, and the specificity of VMI was often significantly less than that of MRI. For parametrial invasion, mean sensitivity, specificity, and AUC for C-CT, VMI, and MRI were 0.81, 0.99, 0.93; 0.64, 0.35, 0.79; and 0.73, 0.67, 0.86, respectively, and MRI had significantly higher specificity and AUC than that of VMI ($p = 0.013$ and 0.008, respectively). Interradiologist agreement was higher for VMI than C-CT and for MRI than VMI.

Conclusion The CNR of VMI was significantly higher than C-CT and interradiologist agreement was better than with C-CT; however, the overall diagnostic performance of VMI did not significantly differ from C-CT and was inferior to MRI. VMI was characterized by low specificity, which should be understood and used for reading.

Keywords
- cervical cancer
- diagnosis
- dual-energy CT
- MRI

DOI https://doi.org/10.1055/s-0044-1787780.
ISSN 0971-3026.

Thieme Medical and Scientific Publishers Pvt. Ltd., A-12, 2nd Floor, Sector 2, Noida-201301 UP, India

Introduction

Cervical cancer is the fourth most common cancer in women, affecting approximately 570,000 individuals and causing 311,000 deaths worldwide in 2018.[1] Patient numbers in developed countries are declining while in developing countries are rapidly increasing.[1] With the revision of the International Federation of Gynecology and Obstetrics (FIGO) 2018, cervical cancer is now staged comprehensively, considering not only physical findings but also imaging.[2,3] Magnetic resonance imaging (MRI) has been used for local diagnosis due to its superior tissue resolution; however, MRI availability is often limited.[4] If computed tomography (CT) can be used for local diagnosis instead of MRI, simultaneous assessment of metastasis becomes possible, leading to shortened treatment time and cost reduction. Low-energy virtual monoenergetic images (VMIs) obtained from dual-energy CT (DECT) improve iodine enhancement in parenchymal tissue and can aid in the detection of various tumors,[5–8] and VMI of 40 keV is reported to have the highest contrast and detection sensitivity. The objective of this study was to assess the effectiveness of 40 keV VMI in the local diagnosis of cervical cancer compared with conventional CT (C-CT) and MRI. The clinicopathologic staging was used as the reference standard for comparison.

Materials and Methods

Study Design

This retrospective study was approved by the Institutional Review Board of our institution, and the need for written informed consent was waived (approval number: R03–117). The inclusion criteria were as follows: (1) histopathologically diagnosed uterine cervical cancer by biopsy and (2) examination using CT and MRI including T1-weighed images (T1WIs), T2-weighted images (T2WI), and diffusion-weighted images (DWIs) performed in our hospital between June 2021 and October 2022.

Patients were excluded if they (1) were not examined by contrast-enhanced DECT or (2) examined by contrast-enhanced DECT with reduced iodine dose. Staging of the uterine cancer was determined by pathology if surgery was performed or by clinical examination (i.e., pelvic examination, cystoscopy, and colposcopy) concerning imaging findings if surgery was not performed.

Image Protocol

All CT examinations were performed using an IQon Spectral CT scanner (Philips Medical Systems, Amsterdam, Netherlands). Scanning was performed with the following acquisition parameters: tube voltage, 120 kVp; helical pitch, 0.798; detector collimation, 64 × 0.625; and rotation time, 0.5 second. Tube current was modulated by automatic exposure control (Dose Right Index, 24–25; Philips Healthcare). A 500 mg/kg dose of contrast medium was injected via a peripheral vein of the upper extremity over 50 seconds using a power injector, followed by a 50-mL saline flush. All scans were captured in a craniocaudal direction from the lung apexes or the hepatic dome to the pubis 80 seconds after intravenous administration of the contrast medium. For image evaluation, images from above the aortic bifurcation to the pubis were selected and reconstructed using C-CT and 40 keV VMI with a slice thickness of 2.0 mm and a reconstruction interval of 2.0 mm. Images of the axial and sagittal planes along the uterine axis were also reconstructed using C-CT and VMI with a slice thickness of 2.0 mm and reconstruction interval of 2.0 mm. Optimal window levels and widths were set at 35 and 350 Hounsfield units (HU) for C-CT, and 140 and 680 HU for VMI.

MRI was performed using 3T or 1.5T equipment (Ingenia, Achieva; Philips Medical Systems, Netherlands). The protocol included T1WI, T2WI, DWI, with a *b*-value of 0 and 1,000, and apparent water diffusion coefficient maps. Further details of these parameters are listed in ►**Table 1**.

Quantitative Image Analysis

Quantitative evaluation of the myometrium and cervical cancer on C-CT and VMI was performed using region-of-interest (ROI) analysis by two board-certified radiologists with 6 years of experience (S.S. and M.Y.). The average of the two measurements was used for the analysis. The mean CT number of the myometrium was measured by placing a circular ROI on the myometrium, carefully avoiding myomas, adenomyomas, and visible vessels. For cervical cancer, the ROI was set to be as large as possible without including the surrounding area. Image noise was quantified as the standard deviation (SD) of the CT number of the anterior

Table 1 Acquisition parameters of MRI

Sequence	Direction	Type	Repetition time/ Echo time (ms)	Flip angle (degree)	Slice/gap (mm)	Field of view (mm)	Matrix
T1WI	Axial (to the pelvis)	3D–GRE	30/2	30	2.4/1.2	280	512
T2WI	Axial (to the pelvis)	3D–TSE	2,000/213	90	1.2/0	280	560
T2WI	Sagittal/axial (to the cervix)	2D–TSE	1,400–6,697/ 10–110	90	3–7/0.3–1	260–380	512 × 512–704 × 704
DWI	Axial (to the cervix)	EPI	4,068–7,500/ 70–79	90	3–7/0–1	260–380	224 × 224–352 × 352

Abbreviations: 3D, three-dimensional; DWI, diffusion-weighted imaging; EPI, echo-planar imaging; GRE, gradient echo; MRI, magnetic resonance imaging; T1WI, T1-weighted imaging; T2WI, T2-weighted imaging; TSE, turbo spin echo.

abdominal wall fat tissue. The signal-to-noise ratio of the myometrium was calculated by dividing the CT number of the myometrium by the image noise. The contrast-to-noise ratio (CNR) of the tumor-to-myometrium was calculated using the following equation: CNR = | (mean HU of myometrium – HU of cervical cancer)/image noise |.[9] Since the enhancing effect of cervical cancer can be weaker or stronger than that of the myometrium, absolute values were used for CNR. Missing values were set in the following conditions: (1) no tumor could be identified, or (2) the tumor replaced the entire uterus, and the myometrium could not be identified.

Qualitative Image Analysis

This study included four board-certified experienced radiologists (K.M., T.S.,T.I., and T.A., and F.F.) with 29, 19, 12, and 7 years of experience in abdominal radiology; they independently reviewed C-CT, VMI, and MRI in random order. They scored each image by assigning the confidence levels for lateral invasion on a 5-point scale (1, tumor not visualized; 2, no parametrial involvement; 3, parametrial involvement; 4, extension to the pelvic wall or hydronephrosis; and 5, bladder or rectum involvement) and the conspicuity of vaginal wall involvement on a 5-point scale (1, tumor not visualized; 2, absent; 3, equivocal; 4, upper two-third involvement; and 5, lower one-third involvement). Regarding the presence of a tumor, a score of 1 for lateral invasion indicated the absence of a tumor, while any score other than 1 was considered as the presence of a tumor. For vaginal involvement, a confidence score of 4 or 5 was considered definitive. The radiologists were blinded to the pathologic and clinical findings, and there was a minimum of 2 weeks between each image set interpretation.

The criteria for local diagnosis on T2WI were as follows: parametrial invasion is excluded if the outer margin of the cervical stroma of low intensity is preserved; parametrial invasion is diagnosed when the following findings are detected: spiculated tumor-to-parametrial interface, tumor nodule in the parametrium, and/or tumor encasement of parametrial vessels. The presence of pelvic wall extension is indicated by tumor extension into the iliac vasculature or muscles including the internal obturator, piriformis, or levator ani. A dilated ureter obstructed by the tumor is also considered a pelvic wall invasion.[10] Bladder/rectal mucosal involvement is diagnosed when the tumor disrupts the low-signal-intensity bladder or rectal wall and extends into the mucosa or lumen.[3] Local staging on imaging was performed according to FIGO 2018: stage I as confined to the cervix; stage II as invasion beyond the uterus without extension to the lower one-third of the vagina or pelvic wall; stage III as invasion of the lower one-third of the vagina/hydronephrosis/nonfunctioning kidney/pelvic wall; and stage IVA as extension beyond the true pelvis or involvement of the bladder or rectum mucosa.[10]

Statistical Analysis

For quantitative analysis, the mean CNR and SD were calculated, and the Wilcoxon signed-rank test was used to evaluate the difference in CNR between C-CT and VMI.

For qualitative analysis, based on the results of the imaging evaluation, the sensitivity, specificity, and accuracy were calculated for the detection of tumor presence, parametrial invasion, pelvic wall extension, bladder/rectum involvement, upper two-third of the vaginal wall involvement, and lower one-third of the vaginal wall involvement; these were calculated by selecting two options of presence or absence. Receiver operating characteristic (ROC) analysis was also performed to evaluate diagnostic performance. The area under the ROC curve (AUC) interpreted the diagnostic value as follows: 0 to 0.70, poor; 0.70 to 0.90, moderate; and 0.90 to 1.00, high.[11] We estimated 95% confidence intervals and performed multiple comparisons using the Friedman test with Bonferroni correction to compare the sensitivity, specificity, accuracy, and AUC. The concordance rate between each reader's C-CT, VMI, and MRI local stage was also calculated. Interobserver agreement was assessed using the κ-statistic. The κ-statistic interpreted the agreement as follows: < 0, none; 0 to 0.20, slight; 0.21 to 0.40, fair; 0.41 to 0.60, moderate; 0.61 to 0.80, substantial; and 0.81 to 1.00, almost perfect.[12] All statistical analyses were performed using the Statistical Package for the Social Sciences software (SPSS Statistics 28.0; IBM, New York, New York, United States). Statistical significance was set at $p < 0.05$.

Results

A total of 33 women (mean age, 56 years; age range, 36–85 years) were evaluated across all the data sets. The flowchart of the study design is shown in ►**Fig. 1**.

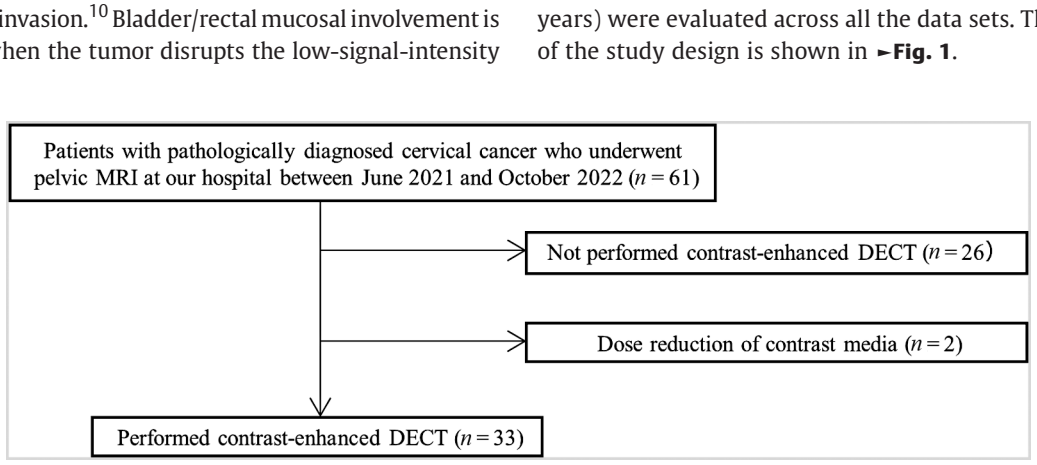

Fig. 1 Flowchart for the patient selection process. DECT; dual-energy computed tomography; MRI, magnetic resonance imaging.

Table 2 Characteristics of patients and lesions

Variable	
Patients (*n*)	33
Age	
Mean ± standard deviation (y)	55 ± 13
Range (y)	36–85
Pathological type (*n*)	
Squamous cell carcinoma	25
Adenocarcinoma	7
Carcinosarcoma	1
Clinical FIGO 2018 Stage (*n*)	
IA/IB1/IB2/IB3	3/1/4/1
IIA/IIB	1/1
IIIA/IIIB/IIIC1/IIIC2	2/6/5/3
IVA/IVB	4/2
Clinicopathologic lateral invasion	
No lateral invasion	13
Parametrial invasion	3
Pelvic wall invasion	13
Bladder/rectal involvement	4
Clinicopathologic vaginal invasion	
No vaginal invasion	15
<Upper two-third vagina	12
>Lower one-third vagina	6

Abbreviation: FIGO, International Federation of Gynecology and Obstetrics.

►**Table 2** shows the patients' characteristics, pathological type, the clinical FIGO 2018 stage, and the clinicopathological invasion. Among the 33 patients, 22 patients were treated with concurrent chemoradiotherapy (CCRT), and the stage was determined clinically; meanwhile, 11 patients underwent a radical hysterectomy, and the stage was determined pathologically. The smallest lesion was 2 mm in depth, as measured by pathology, and the largest lesion was 13 cm in the greatest dimension, as measured by MRI.

Quantitative Image Analysis

In the ROI analysis, three cases with C-CT and two cases with VMI had missing values because cervical cancer could not be identified. In addition, two cases with C-CT and one case with VMI had missing values because the myometrium could not be separated from the tumor. The mean tumor-to-myometrium CNR was 1.57 ± 1.43 on C-CT and 2.73 ± 2.41 on VMI. The mean tumor-to-myometrium CNR was significantly higher on VMI ($p = 0.002$).

Qualitative Image Analysis

All readers rated the image quality of C-CT as "acceptable," "good," or "excellent" and that of VMI and MRI as "good" or "excellent."

The results in ►**Table 3** show variability in sensitivity, specificity, accuracy, and AUC among the different imaging modalities and radiologists. Only cases in which cervical cancer was present were included; therefore, the specificity, accuracy, and AUC were not calculated for the presence of the tumor. In tumor detection, VMI was more sensitive than C-CT in all but one reader and equal to or more sensitive than MRI in all readers. Similarly, in all the other diagnostic parameters, VMI had equal to higher sensitivity than C-CT and MRI, and equal to lower specificity than C-CT and MRI in almost all readers. MRI generally exhibited higher specificity, accuracy, and AUC compared with C-CT and VMI in detecting parametrial invasion and pelvic wall extension. Its sensitivity was higher than that of C-CT, while being comparable to VMI. Additionally, in detecting vaginal wall invasion, even MRI tended to have lower sensitivity and AUC.

►**Table 4** shows readers' mean values of sensitivity, specificity, accuracy, and AUC of each local diagnostic parameter and presents the statistical significance of these differences. Among the parameters, VMI had significantly higher sensitivity than that of C-CT and MRI for the lower one-third vaginal involvement, and VMI was significantly less specific than C-CT for all parameters except bladder/rectum involvement and significantly less specific than MRI for the parametrial invasion and upper two-third vaginal invasion. AUC comparisons showed that MRI was significantly higher than that of VMI for detecting parametrial invasion and pelvic wall extension; however, the other parameters were not significantly different. For parametrial invasion, the most important factor in determining treatment, the positive predictive value (PPV) of each reader was 0.68 to 0.91 for C-CT, 0.67 to 0.77 for VMI, and 0.83 to 0.94 for MRI, and the false positive value (FPV) of each reader was 0.08 to 0.69 for C-CT, 0.46 to 0.77 for VMI, and 0.08 to 0.31 for MRI with lowest for MRI, followed by C-CT and VMI. MRI generally exhibited higher sensitivity, specificity, accuracy, and AUC than C-CT and VMI; however, its diagnostic ability for vaginal wall involvement was inferior to that of lateral extension. Staging accuracy by the four readers was 61, 67, 70, and 39% for C-CT; 55, 70, 64, and 48% for VMI; and 64, 85, 79, and 54% for MRI, respectively.

►**Table 5** shows the interobserver agreement among radiologists in local diagnostic parameters; the interradiologist κ-values for each modality widely ranged, with generally higher agreement for VMI than for C-CT and MRI than for VMI.

►**Figs. 2**–**4** show the C-CT, VMI, and MRI images of IB2, IIA1, and IIIB cervical cancer, respectively. VMI provides better contrast between the uterus and tumor than C-CT, and the tumor is more clearly defined.

Discussion

C-CT, VMI, and MRI were compared to assess the local diagnostic performance of cervical cancer. There was no significant difference in diagnostic performance between C-CT and VMI, with VMI characterized by higher sensitivity, lower specificity, and higher interreader agreement than C-CT.

DECT scanners use more than one peak energy to rapidly acquire images and visualize how tissues and materials

Table 3 Sensitivity, specificity, accuracy, and AUC for local diagnosis parameters of cervical cancer in C-CT, VMI, and MRI by four radiologists

Parameter	Image	Sensitivity	Specificity	Accuracy	AUC
Tumor detection	C-CT VMI MRI	0.87–1.00 0.97–1.00 0.93–1.00			
Parametrial invasion	C-CT	0.40–0.95	0.31–0.92	0.61–0.91	0.63–0.90
	VMI	0.95–1.00	0.23–0.54	0.70–0.81	0.62–0.77
	MRI	0.75–1.00	0.69–0.92	0.81–0.94	0.82–0.92
Pelvic wall extension	C-CT	0.18–0.82	0.50–1.00	0.58–0.85	0.66–0.85
	VMI	0.65–1.00	0.23–0.69	0.64–0.79	0.63–0.78
	MRI	0.53–0.94	0.75–0.88	0.70–0.88	0.70–0.88
Bladder/rectum involvement	C-CT	0.25–1.00	0.93–1.00	0.91–1.00	0.63–1.00
	VMI	0.50–1.00	0.93–0.97	0.88–0.97	0.73–0.98
	MRI	0.50–1.00	0.97–1.00	0.94–1.00	0.75–1.00
Upper two-third vaginal wall involvement	C-CT	0.33–0.94	0.67–0.93	0.58–0.82	0.60–0.81
	VMI	0.56–0.94	0.40–0.67	0.58–0.73	0.58–0.81
	MRI	0.39–0.83	0.67–1.00	0.67–0.79	0.69–0.78
Lower one-third vaginal wall involvement	C-CT	0.17–0.33	0.93–1.00	0.82–0.88	0.50–0.63
	VMI	0.33–0.67	0.74–0.93	0.73–0.85	0.61–0.71
	MRI	0.33–0.55	0.93–1.00	0.85–0.88	0.67–0.73

Abbreviations: AUC, the area under the receiver operating characteristic curve; C-CT, conventional computed tomography; MRI, magnetic resonance imaging; VMI, virtual monoenergetic image.

Table 4 Sensitivity, specificity, accuracy, and AUC for local diagnosis parameters in C-CT, VMI, and MRI

Parameter	Image	Sensitivity	Specificity	Accuracy	AUC	*p* for modality
Tumor detection	C-CT	0.94				Sensitivity: 0.625
	VMI	0.99				
	MRI	0.96				
Parametrial invasion	C-CT	0.81	0.64	0.75	0.73	Sensitivity: 0.670, specificity: 0.013[a] (0.019[a]: C-CT vs. VMI, 0.033: VMI vs. MRI), accuracy: 0.005[a] (0.004[a]: VMI vs. MRI), AUC: 0.042[a] (0.025[a]: VMI vs. MRI)
	VMI	0.99	0.35	0.74	0.67	
	MRI	0.93	0.79	0.87	0.86	
Pelvic wall extension	C-CT	0.63	0.80	0.72	0.72	Sensitivity: 0.867, specificity: 0.013[a] (0.011[a]: C-CT vs. VMI) accuracy: 0.009[a] (0.008[a]: VMI vs. MRI) AUC: 0.008[a] (0.006[a]: VMI vs. MRI)
	VMI	0.82	0.48	0.72	0.71	
	MRI	0.78	0.83	0.81	0.81	
Bladder/rectum involvement	C-CT	0.69	0.98	0.94	0.83	Sensitivity 0.961, specificity: 0.148, accuracy: 0.060, AUC: 0.690
	VMI	0.81	0.94	0.93	0.88	
	MRI	0.81	0.99	0.97	0.90	
Upper two-third vaginal wall involvement	C-CT	0.61	0.79	0.69	0.70	Sensitivity: 0.417, specificity: <0.001[a] (0.043[a]: C-CT vs. VMI, <0.001[a]: VMI vs. MRI), accuracy: 0.809, AUC: 0.819
	VMI	0.79	0.57	0.69	0.68	
	MRI	0.60	0.85	0.72	0.72	
Lower one-third vaginal wall involvement	C-CT	0.29	0.98	0.86	0.60	Sensitivity: 0.002[a] (0.004[a]: C-CT vs. VMI, 0.025[a]: C-CT vs. MRI), specificity: 0.026[a] (0.019[a]: C-CT vs. VMI), accuracy: 0.107, AUC: 0.169
	VMI	0.50	0.84	0.78	0.67	
	MRI	0.46	0.96	0.87	0.71	

Abbreviations: AUC, the area under the receiver operating characteristic curve; C-CT, conventional computed tomography; MRI, magnetic resonance imaging; VMI, virtual monoenergetic image.
[a]$p < 0.05$.

Table 5 Interobserver agreement of local diagnosis parameters between the radiologists

Parameter	C-CT	VMI	MRI
Tumor detection	0.21–0.53 (0.40)	–0.04 to 1.00 (0.37)	0.65–0.87 (0.72)
Parametrial invasion	0.09–0.50 (0.26)	0.31–0.62 (0.50)	0.52–0.86 (0.70)
Pelvic wall extension	0.10–0.33 (0.25)	0.28–0.54 (0.43)	0.35–0.70 (0.55)
Bladder/rectum involvement	0.25–0.77 (0.50)	0.37–0.89 (0.60)	0.53–0.87 (0.60)
Upper two-third vaginal wall involvement	0.17–0.61 (0.34)	0.14–0.58 (0.32)	0.11–0.50 (0.29)
Lower one-third vaginal wall involvement	–0.05–0.28 (0.03)	0.21–0.47 (0.31)	0.43–0.87 (0.62)

Abbreviations: C-CT, conventional computed tomography; MRI, magnetic resonance imaging; VMI, virtual monoenergetic images.
Note: Parentheses indicate the mean.

interact with X-ray beams of different energies. A single DECT acquisition can produce several different image data sets, such as VMIs and material-specific iodine images; these data sets provide superior contrast enhancement and reduce artifacts. Low-energy VMIs (40–55 keV) increase iodine density as they approach the K-edge of iodine (33.2 keV). Improved iodine prominence in low-energy VMI can be useful for tumor detection and characterization, and the use of VMI at the desired energy level (40–140 keV) improves the lesion-to-background contrast and quality of vascular imaging for

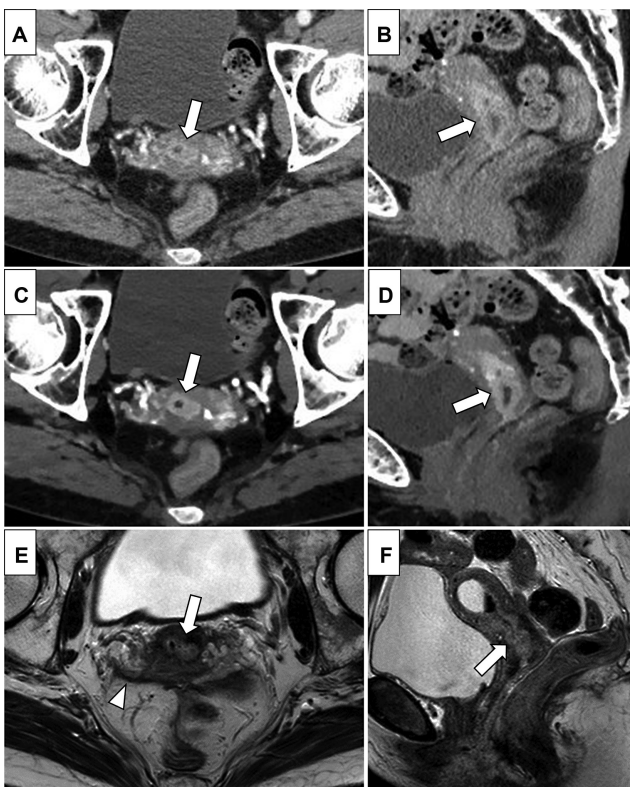

Fig. 2 A 73-year-old female patient with cervical cancer (adenocarcinoma), pathologically diagnosed with International Federation of Gynecology and Obstetrics (FIGO) 2018 IB2. (**A**, **B**) Conventional computed tomography (C-CT) axial, sagittal images. (**C**, **D**) Virtual monoenergetic image (VMI) axial, sagittal images. (**E**, **F**) T2-weighted image (T2WI), sagittal images. C-CT shows a tumor with strong enhancement confined to the cervix (**A**, **B**; arrows). The contrast is accentuated at VMI (**C**, **D**; arrows). On T2WI, the tumor shows high signal intensities (**E**, **F**; arrows). On C-CT, one reader could not detect the tumor. On VMI, all readers made the correct diagnosis. On magnetic resonance imaging (MRI), three readers overdiagnosed as extending to the pelvic wall with involvement of the vaginal wall (**E**; arrowhead, which is considered a combination of vascular and peritoneal thickening).

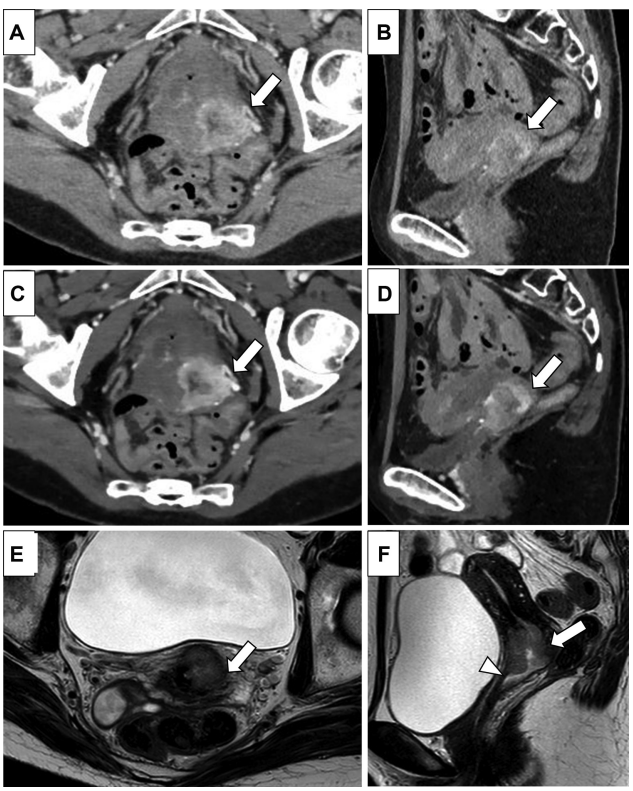

Fig. 3 A 56-year-old female patient with cervical cancer (squamous cell carcinoma), pathologically diagnosed with International Federation of Gynecology and Obstetrics (FIGO) 2018 IIA1. (**A**, **B**) Conventional computed tomography (C-CT) axial, sagittal images. (**C**, **D**) Virtual monoenergetic image (VMI) axial, sagittal images. (**E**, **F**) T2-weighted image (T2WI) axial, sagittal images. The tumor is strongly enhanced, predominantly at the margins on C-CT (**A**, **B**; arrows). On VMI, the tumor enhancement effect is stronger, and its margins are more clearly defined (**C**, **D**; arrows). The preserved outer rim of cervical stroma on T2WI indicates no parametrial invasion (**E**; arrow), and the tumor reaches the upper edge of the anterior vaginal wall (**F**; arrowhead). On C-CT, one reader failed to detect the tumor. On VMI, three readers overdiagnosed with extension to the pelvic wall, but three readers correctly diagnosed the upper two-third vaginal involvement. On magnetic resonance imaging (MRI), only half of the readers correctly diagnosed lateral and vaginal invasion.

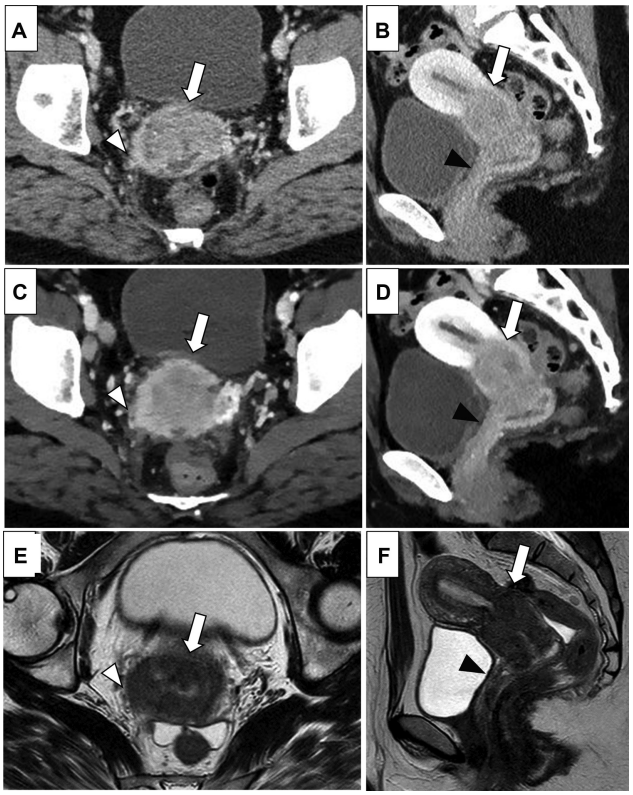

Fig. 4 A 38-year-old female patient with cervical cancer (squamous cell carcinoma), clinically diagnosed with International Federation of Gynecology and Obstetrics (FIGO) 2018 IIIB. (**A**, **B**) Conventional computed tomography (C-CT) axial, sagittal images. (**C**, **D**) Virtual monoenergetic image (VMI) axial, sagittal images. (**E**, **F**) T2-weighted image (T2WI) axial, sagittal images. The tumor shows relative hypoattenuation with strongly enhanced margins (**A**–**D**; arrows), predominantly reaching the right pelvic wall (**A**, **C**; arrowheads) and invading the upper two-third vaginal wall (**B**, **D**; black arrowheads) on CT. T2WI showing spiculated tumor-to-parametrial interface reaching the iliac vasculature (**E**; arrowhead), and thickening of the anterior vaginal wall (**F**; black arrowhead). On C-CT, only one reader misdiagnosed as no parametrial invasion, and all the readers correctly diagnosed vaginal invasion. On VMI, half of the readers overdiagnosed with bladder and rectal involvement, as well as the lower one-third vaginal involvement. On magnetic resonance imaging (MRI), all readers correctly diagnosed lateral invasion, but only one reader correctly diagnosed vaginal invasion.

preoperative planning. Lv et al reported that the lesion detectability and conspicuity of small hepatocellular carcinoma could be improved by selecting the optimal energy level (40–70 keV) for monochromatic imaging.[6] De Cecco et al reported that the diagnostic accuracy in detecting hypervascular liver lesions is improved with 40 keV VMI.[13] Nagayama et al demonstrated that VMI yielded significantly better image quality in multiphasic pancreatic CT than conventional polyenergetic images. In each enhancement phase, 40 keV VMI provided the best quality for the evaluation of pancreatic duct cancer owing to its high pancreas-tumor contrast and vascular opacification without a relevant increase in image noise.[7] For uterus tumors, Rizzo et al evaluated deep (> 50%) myometrial invasion using DECT and transvaginal ultrasound in patients with endometrial cancer, and reported that low keV VMI showed higher specificity and accuracy than that of ultrasound.[14] To the best of our knowledge, there have been no DECT studies of uterine cervical cancer, and including other tumors, few studies have evaluated the utility of DECT in assessing the surrounding invasion of tumors.

For the staging of cervical cancer, the role of imaging is to evaluate invasion to the parametrium, pelvic wall, and adjacent organs and the assessment of nodal involvement and distant metastasis. The strength of MRI in diagnosing cervical cancer is the high negative predictive value (NPV) of 95% in detecting parametrial invasion,[15,16] and Manganaro et al have documented a 100% NPV of MRI for bladder or rectal invasion, suggesting that MRI can obviate invasive procedures, such as cystoscopy, proctoscopy, and sigmoidoscopy.[3] The reported accuracy for the parametrial invasion was 70 to 80% on CT and 87 to 92% on MRI in the 1990s.[17,18] Moreover, the reported sensitivity, specificity, PPV, and NPV were 0.42 to 0.50, 0.75 to 0.82, 0.33 to 0.53, and 0.67 to 0.84 for CT, respectively; and 0.53 to 0.67, 0.67 to 0.75, 0.37 to 089, and 0.85 to 0.92 for MRI, respectively.[18–20] The overall staging accuracy of MRI reported between 1988 and 2003 was 76 to 86%, higher than that of CT at 53 to 69%.[15,17,18,21]

In recent years, there have been few reports on the pathological image correlation beyond stage II in cervical cancer cases, mainly due to the fact that stage IB3 (tumor larger than 4 cm) and higher are typically managed with CCRT. A multicenter study conducted in 2005, focusing on early-stage invasive cervical cancer, found that the accuracy and specificity of both CT and MRI in assessing parametrial involvement and overall staging were quite similar; however, the accuracy of both modalities was relatively low, while the specificity was high.[20] A meta-analysis of the literature between 2012 and 2016 has revealed that the sensitivity and specificity of MRI in detecting parametrial invasion, using radical hysterectomy as the reference standard, were 76 and 94%, respectively.[21] Similar to our study, Yu et al using clinicopathologic staging as a reference and covering all stages, reported that the accuracy of stage classification of cervical cancer in a single facility from 2010 to 2015 was 80% for MRI and 73% for CT, showing a significant difference.[22] As the majority of studies indicate, MRI has consistently shown significantly higher accuracy compared with CT.

Conventionally, low-energy images have high noise and contrast, whereas high-energy images have low noise and contrast. However, in our study, by setting the optimal window width and window level during reconstruction, all readers rated the image quality of VMI as good or excellent, and the noise was less noticeable than that of C-CT, similar to a previous report.[7] The diagnostic performance of VMI was not significantly different from that of C-CT in all the diagnostic parameters and was inferior to MRI in the parametrial invasion and the pelvic extension; however, in VMI, the tumor became more distinct due to increased contrast between the tumor and background with a significantly higher CNR than C-CT, leading to improved diagnostic sensitivity, actually, with one-third vaginal involvement, VMI was significantly more sensitive than C-CT. It was also believed that this facilitated easier interpretation, increasing readers' agreement rates. Although

not verified in this study, there may have been differences in diagnostic confidence and reading time. On the other hand, the specificity of VMI was significantly lower than that of C-CT and MRI, and VMI had a lower PPV. This is due to the higher FPV of VMI because of the accentuated heterogeneity of the cervical stroma, myometrium, and vaginal wall enhancement. Additionally, the current reading method was developed using C-CT, which was a disadvantage for VMI. Radiologists usually use MRI, not CT, for diagnosing cervical cancer. The FIGO clinical stage often depends on MRI findings, which puts CT at a disadvantage. Previous reports have shown an accuracy of 74 to 93% for vaginal invasion on MRI,[15,23] but in the present study, the diagnostic performance of MRI for vaginal wall invasion was lower than for lateral invasion. This could be improved by adding the sagittal section of DWI,[24] vaginal opacification,[21] or dynamic contracted-enhanced MRI which remains an option in the European Union Special Representatives guidelines. In dynamic contrast-enhanced MRI, cervical cancer typically shows early enhancement with hyperintensity relative to normal cervical stroma in the arterial phase making tumor detection easier.[23] This effect is particularly considered useful in detecting small tumors.[25] However, the role of imaging in evaluating vaginal involvement may be limited because it is usually clinically assessed. In the case of an exophytic tumor, the vaginal fornix adjacent to the mass appears thin because they are stretched by the tumor, making it difficult to distinguish the thin vaginal fornix from the adjacent tumor; additionally, 39% of the cases in this study had superficial spreading detected only using the Schiller test, which is considered difficult to capture on imaging. The overall staging accuracy in our study was 39 to 70% for C-CT, 48 to 70% for VMI, and 54 to 85% for MRI, which is generally consistent with previous studies, although there are large individual differences.

This study had several limitations. First, the number of patients was small. Second, CCRT is the standard treatment for stage IB3 or higher cervical cancer; therefore, the reference standard of parametrial, pelvic wall, and vaginal invasion was based on clinical examination concerning imaging findings in two-thirds of the cases. Third, because only cervical cancer cases were included in the study, a blinded evaluation of the tumor detection power was not possible. Finally, only 40 keV VMI was used because it was considered to have the highest contrast in previous reports; other low-energy VMIs were not evaluated.

In conclusion, there was no significant difference in diagnostic performance between C-CT and VMI in the local diagnosis of cervical cancer. However, virtual monoenergetic imaging demonstrated a significantly higher tumor-to-myometrial contrast ratio, higher sensitivity, and greater inter-reader agreement. Conversely, these images were associated with lower specificity. These characteristics should be understood and utilized in CT reading and experience should be accumulated.

Authors' Contributions

T.S.: Methodology, formal analysis, and investigation.
S.S.: Writing – original draft preparation.
S.S.,T.S., K.M., T.I., T.A., M.Y., M.M.,T.S., and T.N.: Writing – review and editing.
T.S., K.M.,T.I., T.A., M.Y., M.M., and T.S.: Resources.
T.N.: Supervision.

Funding

The funding for this article was provided by Bayer Academic Support (grant no.: BASJ20220418025).

Conflict of Interest

None declared.

References

1 Sung H, Ferlay J, Siegel RL, et al. Global cancer statistics 2020: GLOBOCAN estimates of incidence and mortality worldwide for 36 cancers in 185 countries. CA Cancer J Clin 2021;71(03):209–249
2 Lee SI, Atri M. 2018 FIGO staging system for uterine cervical cancer: enter cross-sectional imaging. Radiology 2019;292(01):15–24
3 Manganaro L, Lakhman Y, Bharwani N, et al. Staging, recurrence and follow-up of uterine cervical cancer using MRI: updated guidelines of the European Society of Urogenital Radiology after revised FIGO staging 2018. Eur Radiol 2021;31(10):7802–7816
4 OECD (2024), Computed tomography (CT) scanners. doi: 10.1787/bedece12-en
5 Agrawal MD, Pinho DF, Kulkarni NM, Hahn PF, Guimaraes AR, Sahani DV. Oncologic applications of dual-energy CT in the abdomen. Radiographics 2014;34(03):589–612
6 Lv P, Lin XZ, Chen K, Gao J. Spectral CT in patients with small HCC: investigation of image quality and diagnostic accuracy. Eur Radiol 2012;22(10):2117–2124
7 Nagayama Y, Tanoue S, Inoue T, et al. Dual-layer spectral CT improves image quality of multiphasic pancreas CT in patients with pancreatic ductal adenocarcinoma. Eur Radiol 2020;30(01):394–403
8 Foti G, Ascenti G, Agostini A, et al. Dual-energy CT in oncologic imaging. Tomography 2024;10(03):299–319
9 Noda Y, Tochigi T, Parakh A, Joseph E, Hahn PF, Kambadakone A. Low keV portal venous phase as a surrogate for pancreatic phase in a pancreatic protocol dual-energy CT: feasibility, image quality, and lesion conspicuity. Eur Radiol 2021;31(09):6898–6908
10 Balcacer P, Shergill A, Litkouhi B. MRI of cervical cancer with a surgical perspective: staging, prognostic implications and pitfalls. Abdom Radiol (NY) 2019;44(07):2557–2571
11 Linden A. Measuring diagnostic and predictive accuracy in disease management: an introduction to receiver operating characteristic (ROC) analysis. J Eval Clin Pract 2006;12(02):132–139
12 Landis JR, Koch GG. The measurement of observer agreement for categorical data. Biometrics 1977;33(01):159–174
13 De Cecco CN, Caruso D, Schoepf UJ, et al. A noise-optimized virtual monoenergetic reconstruction algorithm improves the diagnostic accuracy of late hepatic arterial phase dual-energy CT for the detection of hypervascular liver lesions. Eur Radiol 2018;28(08):3393–3404
14 Rizzo S, Femia M, Radice D, et al. Evaluation of deep myometrial invasion in endometrial cancer patients: is dual-energy CT an option? Radiol Med (Torino) 2018;123(01):13–19
15 Togashi K, Nishimura K, Sagoh T, et al. Carcinoma of the cervix: staging with MR imaging. Radiology 1989;171(01):245–251
16 Hricak H, Powell CB, Yu KK, et al. Invasive cervical carcinoma: role of MR imaging in pretreatment work-up–cost minimization and diagnostic efficacy analysis. Radiology 1996;198(02):403–409
17 Kim SH, Choi BI, Han JK, et al. Preoperative staging of uterine cervical carcinoma: comparison of CT and MRI in 99 patients. J Comput Assist Tomogr 1993;17(04):633–640
18 Kim SH, Choi BI, Lee HP, et al. Uterine cervical carcinoma: comparison of CT and MR findings. Radiology 1990;175(01):45–51

19 Hancke K, Heilmann V, Straka P, Kreienberg R, Kurzeder C. Pretreatment staging of cervical cancer: is imaging better than palpation?: Role of CT and MRI in preoperative staging of cervical cancer: single institution results for 255 patients Ann Surg Oncol 2008;15(10):2856–2861
20 Hricak H, Gatsonis C, Chi DS, et al; American College of Radiology Imaging Network 6651 Gynecologic Oncology Group 183. Role of imaging in pretreatment evaluation of early invasive cervical cancer: results of the intergroup study American College of Radiology Imaging Network 6651-Gynecologic Oncology Group 183. J Clin Oncol 2005;23(36):9329–9337
21 Woo S, Suh CH, Kim SY, Cho JY, Kim SH. Magnetic resonance imaging for detection of parametrial invasion in cervical cancer: an updated systematic review and meta-analysis of the literature between 2012 and 2016. Eur Radiol 2018;28(02):530–541
22 Yu L, Zhang HF, Jiang DW, Zhao DY, Liu H, Shen LM. Comparison of imaging features and diagnostic values of MRI, CT and contrast-enhanced ultrasonography in the diagnosis of cervical carcinoma staging. Eur Rev Med Pharmacol Sci 2018;22(15):4784–4791
23 Hricak H, Lacey CG, Sandles LG, Chang YC, Winkler ML, Stern JL. Invasive cervical carcinoma: comparison of MR imaging and surgical findings. Radiology 1988;166(03):623–631
24 Park JJ, Kim CK, Park SY, Park BK. Parametrial invasion in cervical cancer: fused T2-weighted imaging and high-b-value diffusion-weighted imaging with background body signal suppression at 3 T. Radiology 2015;274(03):734–741
25 Huang JW, Song JC, Chen T, Yang M, Ma ZL. Making the invisible visible: improving detectability of MRI-invisible residual cervical cancer after conisation by DCE-MRI. Clin Radiol 2019;74(02):166.e15–166.e21

